COBEM 2021 26th International Congress of Mechanical Engineering
November 22-26, 2021, Virtual Congress, Brazil

COBEM2021-2336
ELASTIC WAVE BAND GAPS IN 2D FRACTAL PHONONIC CRYSTALS

Victor Gustavo Ramos Costa Dos Santos[1]
José Maria Campos Dos Santos[2]
University of Campinas, UNICAMP-FEM-DMC, Rua Mendeleyev, 200, CEP 13083-970, Campinas, SP, Brasil
v228253@dac.unicamp.br[1];
zema@unicamp.br[2];

Edson Jansen Pedrosa de Miranda Jr.[3]
Federal Institute of Maranhão, IFMA-PPGEM, Avenida Getúlio Vargas, 4, CEP 65030-005, São Luís, MA, Brasil
University of Campinas, UNICAMP-FEM-DMC, Rua Mendeleyev, 200, CEP 13083-970, Campinas, SP, Brasil
edson.jansen@ifma.edu.br[3]

Abstract. *The wave propagation in a 2D fractal phononic crystal solid is investigated. This special type of phononic crystal is capable of filtering elastic waves in multiple ranges of frequency, called band gaps. The band structures are obtained by the plane wave expansion (PWE) approach considering wave propagation in the xy plane in order to obtain the propagating modes. The multiple Bragg-type band gaps between XY and Z modes are opened up in different frequency bands depending on the fractal order. This fractal order influences significantly the band gap positions and widths. The results can be used for elastic wave attenuation using 2D fractal periodic structures.*

Keywords: *periodicity, vibration control, multiple band gaps.*

1. INTRODUCTION

Recently, there has been growing interest in synthetic materials, also known as phononic crystals (PCs) in many acoustic and structural problems. PCs are constituted from two or more materials with wide difference between their properties, these property contrasts creates band gaps in the frequency response. Currently, they can be used in many applications such as noise and vibration control, filters, resonators, and acoustic waveguides. PCs are periodic structures and it is natural to choose a unit to represent the entire infinite domain.The Floquet-Bloch theorem can be easily used in this type of structure, as there are periodic boundary conditions. Therefore, initially, this article is based on the study of the unit cell structure and its division into fractals of up to third stage (or second iteration, Fig. 1).

Various methods have been developed in order to evaluate band structures of PCs, the Boundary Element Method (BEM) was used by Li *et al.* (2018), H. Page *et al.* (2005) used the Multiple Scattering Theory (MST) to tune and determine the dispersion of ultrasonic pulses in 3D PCs. Vasseur *et al.* (1994) and Yao *et al.* (2009) applied Plane Wave Expansion (PWE) for different types of thin plate defects and supercell arrangement configuration alternatives, the PWE also is used for calculate band structures for fractals phononic crystals, as seen in the work of Huang *et al.* (2017).

Two-dimensional metamaterials are composed of plates with resonant cylinders, which have been shown to attenuate waves much larger than their characteristic unit cell size, thereby opening the wavelength band gap. However, the gap bandwidth is closely related to the quality of the resonator, which limits the function of metamaterials in mass-sensitive applications (Bilal *et al.*, 2017). In order to overcome this limitation, Bilal *et al.* (2017) theoretically shows that the trampoline phenomenon expands the width of the first part of the gap to 4 times the linear resonance gap. They provided an experimental demonstration of the trampoline phenomenon on a 3D printed board composed of pillars and holes made of a single material. They show through numerical and experimental results that the trampoline board increases the width of the partial and full bandwidth range, while reducing the mass of the board by about 30% in the configuration studied.

In this paper, we will approach the structures with traditional fractal geometry that, due to their exact self-similarity, are called deterministic fractals. By exact self-similarity is meant the no change of the structure after an isotropic transformation, that is, which occurs with the same intensity in all directions. For example, consider a fractal called Sierpinski's triangle (base geometry of traditional fractals), as shown in Fig. 1 (a). Its basic structure starts with a completely filled equilateral triangle. At first, take the midpoint of the three sides and form four congruent triangles with the vertices of the original triangle. Then, the center triangle is removed, completing the first stage of the basic construction process. This undo will produce three congruent triangles whose sides are half the sides of the original triangle. Repeat the above process for each of these three triangles. Repeat the same process for the obtained triangles (Assis, 2008; Kuo and Piazza, 2011).

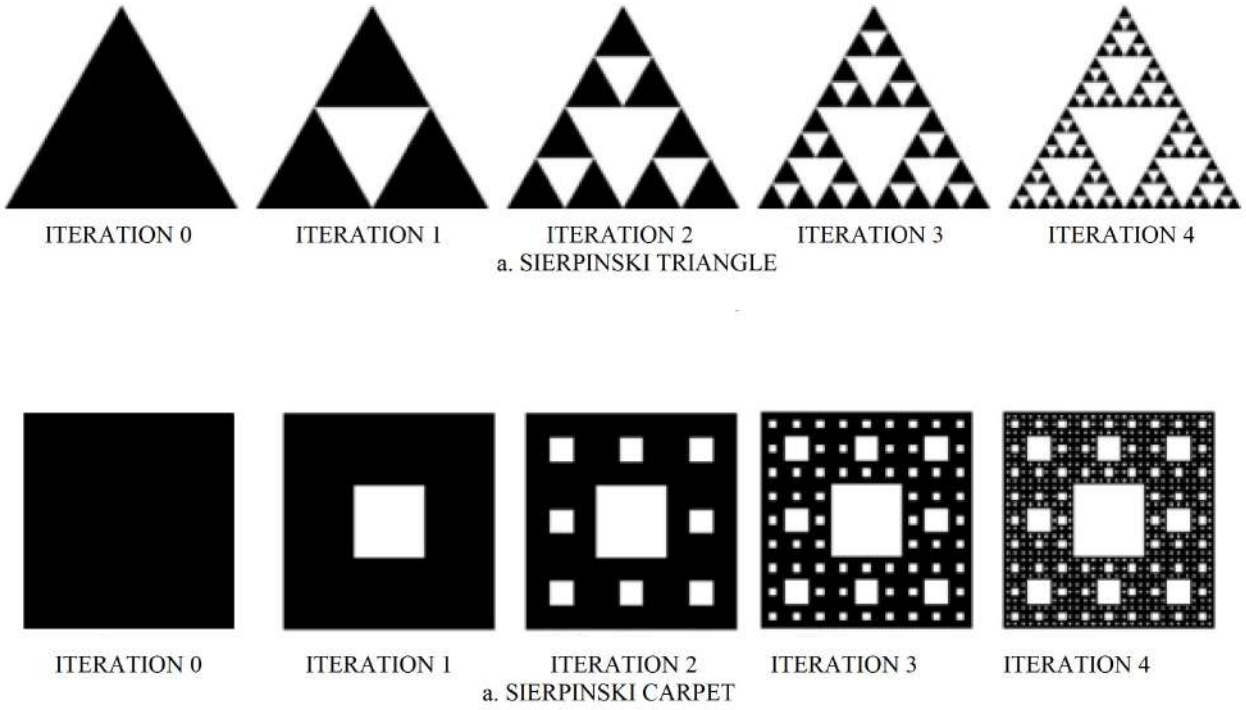

Figure 1. Distribution strategy of self-similar fractals for the generation of PCs. Reprinted [adapted] from Reha and Bouchouirbat (2018).

For the implementation of PCs in this work, we used fractals quasi-Sierpinski carpet and an adapted version of the distribution for square and circular inclusions.

2. MATHEMATICAL FORMULATION

2.1 Plane Wave Expansion

This section presents briefly the PWE formulation for a 2D PC thin plate and the fractals distribution parameters, more details can be found in references Vasseur *et al.* (1994) and Huang *et al.* (2017). The PC shown the scheme including geometric for square and circular cross-section for the inclusions, presented in Fig. 2(a-b). It is an infinite periodic array of inclusions attached periodically in a host matrix made with isotropic materials. The PWE method is used to determine band structure, also known as dispersion relation. The wave propagation is restricted to the plane $(x - y)$, the system is obtained solving the eigenvalue problem only for First Irreducible Brillouin Zone (FIBZ) (Fig. 2(c)).

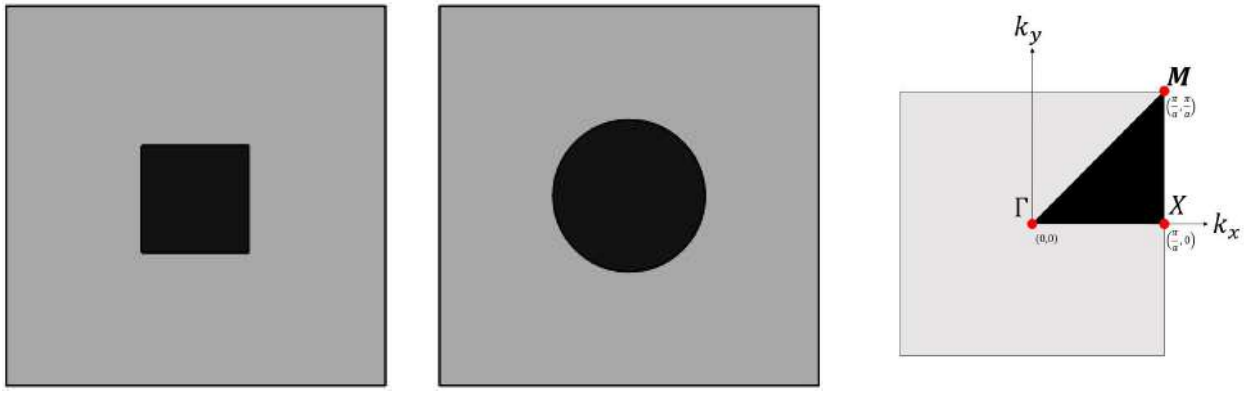

(a) (b) (c)

Figure 2. (a) Square and (b) circular cross section for iteration 1 in fractal quasi-Sierpinski ; (c) First irreducible Brillouin zone (FIBZ).

The govern differential equation for a bending thin plate with uniform thickness is given by Sigalas and Economou (1992):

$$-\alpha\frac{\partial^2 w}{\partial t^2} = \frac{\partial^2}{\partial x^2}\left(D\frac{\partial^2 w}{\partial x^2} + \beta\frac{\partial^2 w}{\partial y^2}\right) + 2\frac{\partial^2}{\partial x \partial y}\left(\gamma\frac{\partial^2 w}{\partial x \partial y}\right) + \frac{\partial^2}{\partial y^2}\left(D\frac{\partial^2 w}{\partial y^2} + \beta\frac{\partial^2 w}{\partial x^2}\right), \tag{1}$$

where w is the transverse displacement in the z-direction, $D = \frac{Eh^3}{12(1-\nu^2)}$ is the flexural rigidity with E being the Young's modulus and ν is the Poisson's ratio. The other parameters are given by $\alpha = \rho h$, $\beta = D\nu$, and $\gamma = D(1-\nu)$. These parameters are periodic functions of the position vector $\mathbf{r}(x, y)$. Using Floquet-Bloch's theorem, the displacement fields of flexural waves in the PC thin plate can be expressed as:

$$w(\mathbf{r}, t) = e^{j(\mathbf{k}\cdot\mathbf{r} - \omega t)} w_{\mathbf{k}}(r), \tag{2}$$

where $\mathbf{k} = (k_x, k_y)$ is the Bloch wave vector, ω is the angular frequency, t is the time and $j = \sqrt{-1}$. The parameter $w_{\mathbf{k}}$ is a periodic function with the same spatial periodicity as the structure and can be expanded in Fourier series as

$$w_{\mathbf{k}} = \sum_{\mathbf{g}_1} e^{j\mathbf{g}_1\cdot\mathbf{r}} A_{\mathbf{g}_1}, \tag{3}$$

where $\mathbf{g}_1 = \frac{2\pi}{a}(n_1, n_2)$ is 2D reciprocal lattice vector for square lattice with n_1 and n_2 ranging from $0, \pm1, \pm2, ..., \pm n$, a is the lattice parameter and $A_{\mathbf{g}_1}$ is the corresponding Fourier coefficient.

The plate parameters, $\alpha(\mathbf{r})$, $\beta(\mathbf{r})$, $D(\mathbf{r})$ and $\gamma(\mathbf{r})$, also expand in a Fourier series as:

$$H(\mathbf{r}) = \sum_{\mathbf{g}_2} e^{j\mathbf{g}_2\cdot\mathbf{r}} H_{\mathbf{g}_2}, \tag{4}$$

where $H(\mathbf{r})$ is only one plate parameters and the corresponding Fourier coefficient is given by:

$$H_{\mathbf{g}_2} = \begin{cases} fH_A + (1-f)H_B & for \quad \mathbf{g}_2 = \mathbf{0} \\ (H_A - H_B)F_{\mathbf{g}_2} & for \quad \mathbf{g}_2 \neq \mathbf{0} \end{cases}, \tag{5}$$

where $\mathbf{g}_2 = \frac{2\pi}{a}(\bar{n}_1, \bar{n}_2)$, with $\bar{n}_1$ and $\bar{n}_2$ range from $0, \pm1, \pm2, ..., \pm n$, $H_{\mathbf{g}_2}$ refers to a Toeplitz matrix. The function f is defined as the ratio between the cross sectional area of a cylinder and primitive unit cell, i.e., filling fraction of each inclusion. $F_{\mathbf{g}_2}$ is the structure function, defined as:

$$F_{\mathbf{g}_2} = \frac{1}{S}\int_S e^{-j\mathbf{g}\cdot\mathbf{r}} dr^2, \tag{6}$$

where S refers to the area of the unit cell and the integral operator being calculated over the cross section of the material A.

1. For circular cylinder inclusions with radius r_o, we have:

$$f = \frac{\pi r_o^2}{a^2} \quad \text{and} \quad F_{\mathbf{g}_2} = \frac{2f}{|\mathbf{g}_2| r_o} J_1(|\mathbf{g}_2| r_o) \ , \tag{7}$$

   with $J_1(|\mathbf{g}_2| r_o)$ is the Bessel function of the first kind.

2. For square section of width $2 \cdot l$

$$f = \frac{2l^2}{a^2} \quad \text{and} \quad F_{\mathbf{g}_2} = f\frac{\sin(g_1 l)}{(g_1 l)} \cdot \frac{\sin(g_2 l)}{(g_2 l)} \ , \tag{8}$$

Substituting Eqs. (2) - (4) in Eq. (1), after some mathematical manipulations, we can express the following eigenvalue problem:

$$\begin{aligned} \omega^2 \sum_{\mathbf{g}_1} [\alpha]_{\mathbf{g}_2} A_{\mathbf{k}+\mathbf{g}_1} \quad = \quad & \sum_{\mathbf{g}_1} (\mathbf{k}+\mathbf{g}_1)_x^2 (\mathbf{k}+\mathbf{g}_3)_x^2 [D]_{\mathbf{g}_2} A_{\mathbf{k}+\mathbf{g}_1} + \\ + \quad & \sum_{\mathbf{g}_1} (\mathbf{k}+\mathbf{g}_1)_y^2 (\mathbf{k}+\mathbf{g}_3)_x^2 [\beta]_{\mathbf{g}_2} A_{\mathbf{k}+\mathbf{g}_1} + \\ + \quad & 2\sum_{\mathbf{g}_1} (\mathbf{k}+\mathbf{g}_1)_x (\mathbf{k}+\mathbf{g}_1)_y (\mathbf{k}+\mathbf{g}_3)_x (\mathbf{k}+\mathbf{g}_3)_y [\gamma]_{\mathbf{g}_2} A_{\mathbf{k}+\mathbf{g}_1} + \\ + \quad & \sum_{\mathbf{g}_1} (\mathbf{k}+\mathbf{g}_1)_y^2 (\mathbf{k}+\mathbf{g}_3)_y^2 [D]_{G_2} A_{\mathbf{k}+\mathbf{g}_1} + \\ + \quad & \sum_{\mathbf{g}_1} (\mathbf{k}+\mathbf{g}_1)_x^2 (\mathbf{k}+\mathbf{g}_3)_y^2 [\beta]_{\mathbf{g}_2} A_{\mathbf{k}+\mathbf{g}_1}, \end{aligned} \tag{9}$$

where $\mathbf{g}_3 = \mathbf{g}_1 + \mathbf{g}_2$. Furthermore, Eq. (9) can be rewritten in a matrix form:

$$\omega^2 P A_{k+g_1} = Q A_{k+g_1}, \tag{10}$$

where ω is the eigenfrequency and can be obtained by solving Eq. (10) for each real value of Bloch vector **k** within FIBZ. Yao *et al.* (2009) and Vasseur *et al.* (1994) show more details for deriving this formulation.

The squared unit cell center (size a) is the coordinate origin. The number of grids for the L-stage is $N = M^{2L}$, where M is the initial grid number of the 1st-stage, and K is the number of gray sub-squares in the x or y direction. For the gray sub-squares in the central scatter, the central position of each sub-square can be defined as $\mathbf{r}_i = r_b + \frac{a}{M^L}(s-1),\ s = 1, ..., KM^{L-1}$, where $i = x, y$; $r_b = a(1 - KM^{L-1})/2M^L$ represents the initial position of the first scale. Fig. 3 showns the scheme example for distribution and positioning of fractals from the second stage.

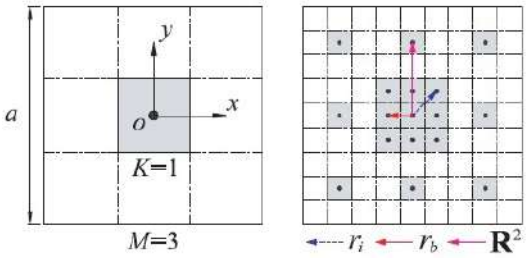

Figure 3. Distribution and positioning of fractals from the second stage. Reprinted [adapted] from Huang *et al.* (2017).

2.2 Band Structures for PCs

We calculate first the band structure of a PC thin plate composed by square section (Fig. 2 a). Single unit cell was calculated with 441 plane waves ($-10 \leq n_{x,y} \leq 10$). For the other cases, we use the supercell method linked at PWE composed by 3×3 square inclusions and 1089 plane waves ($-16 \leq n_{x,y} \leq 16$) (i.e., when we implement the cases for stages 2 and 3 of fractals). The next steps consist of evaluating each iteration of fractal distribution and the influence along the PC band structures.

(a) (b)

Figure 4. Iteration 1 and 2 in fractal quasi-Sierpinski for inclusions: (a) square and (b) cylinder.

3. SIMULATED RESULTS

The results found in Liu *et al.* (2007) and Huang *et al.* (2017) were replicated in the commercial finite element (FE) software COMSOL (·) and compared with those obtained by the implementation of the PWE (o) method proposed in this work and used for the phononic crystal case based on the Sierpinski carpet plane fractal in the first stage. The material parameters used in this article are listed in Tab. 1. The results are shown in Fig. 5. In the initial analysis, the PWE method was implemented only for a first-stage quasi-Sierpinski fractal, and will be implemented in the future for stages 2 and 3 of the fractal.

Table 1. Material properties

Material	Density [kg/m^3]	Young's Modulus [GPa]
Rubber	1,300	1.175
Pb	11,600	40

The convergence between the modes seen in the band structure calculated by PWE is very good when observing the first modes calculated by FEM in COMSOL (Fig. 5). However, as the frequency increases, it can be observed that the answers found no longer overlap. We use 441 plane waves are used in the following calculations. For low frequencies,

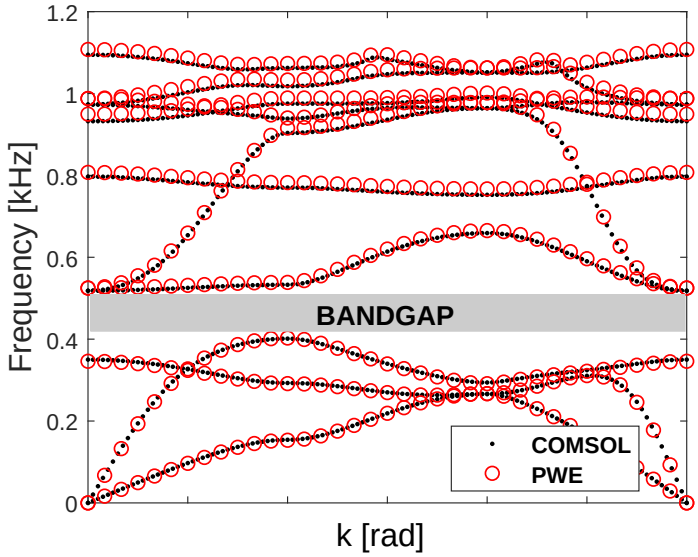

Figure 5. Band structure comparison between COMSOL FEM and PWE of PC fractal with quasi-Sierpinski distribution for square inclusions.

up to 800 Hz, we found a good convergence. However, from 1000 Hz forward, there is already a small shift between responses.

The band structure shown in Fig. 6 was calculated only via finite elements, where we evaluate the behavior of the PC from filling fraction increase from the variation of stages 1, 2 and 3 of the Sierpinski carpet. The bandgaps of the structure bands are easily verified by increasing the fill fraction. Thus, a first full bandgap appears at frequency ranging from 380 to 560 Hz (Fig. 6 (a)).

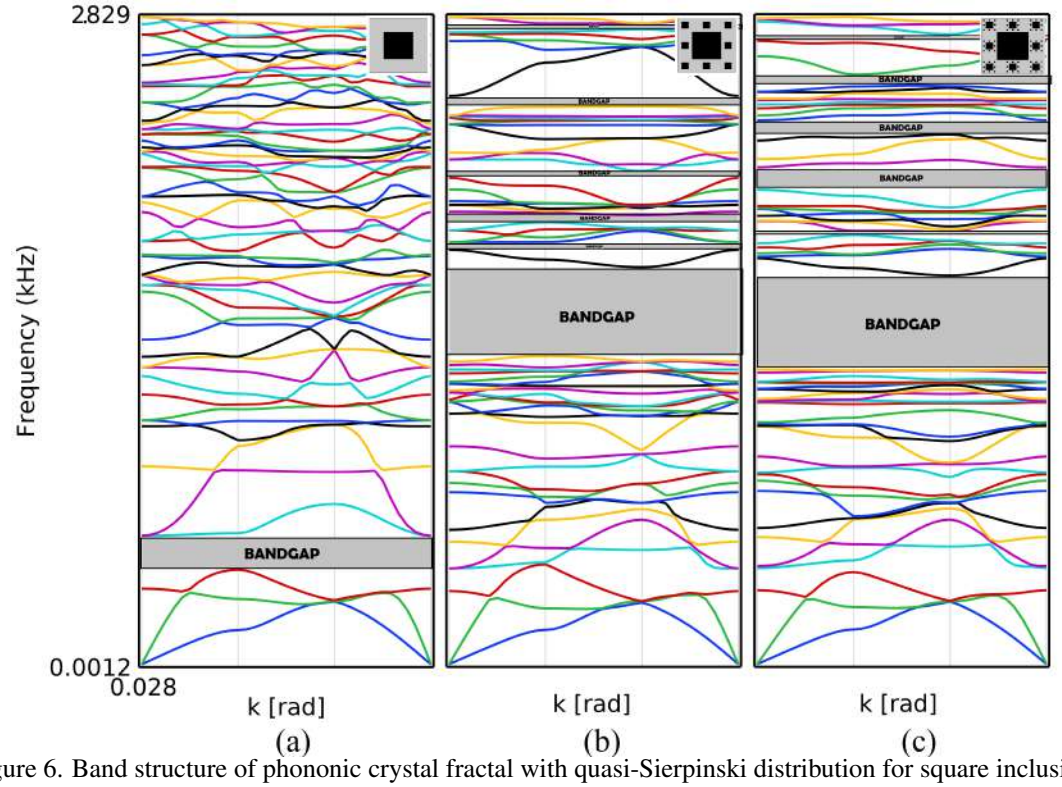

Figure 6. Band structure of phononic crystal fractal with quasi-Sierpinski distribution for square inclusions.

In Fig. 6 (b), the first bandgap that appeared at low frequency does not exist and one large full-band gaps appeared in the middle frequency range of 1335 to 1708 Hz. In addition to this wider bandgap, it was also possible to observe the appearance of five more bandgaps with a small bandwidth, in the region of highest frequencies 1935, 2172, 2576 and 2785 Hz. On the third stage PC, in general, there was a small increase in the first bandwidth gap. The five bandgaps that

appeared in the second stage were also found here. However, the bandgaps that existed in the mid/high frequency range also had an increase in the frequency range where wave propagation attenuation occurs: 2009, 2894, 2468, 2655, and 2702 Hz.

As the first stage presented for the PC with square inclusion, as the initial filling fraction was the same, the response for the circular case is similar, presenting the first complete bandgap in the frequency range ranging from 395 to 577 Hz (Fig. 7 (a)). In Fig. 7 (b), the first bandgap that appeared at low frequency does not exist and two large full-band gaps appeared in the middle frequency range of 1410 to 1590 Hz and 1895 to 2087 Hz. In addition to these two wider bandgaps, it was also possible to observe the appearance of four more bandgaps with a small bandwidth, in the frequencies of 935, 1220, 1700 and 2576 Hz.

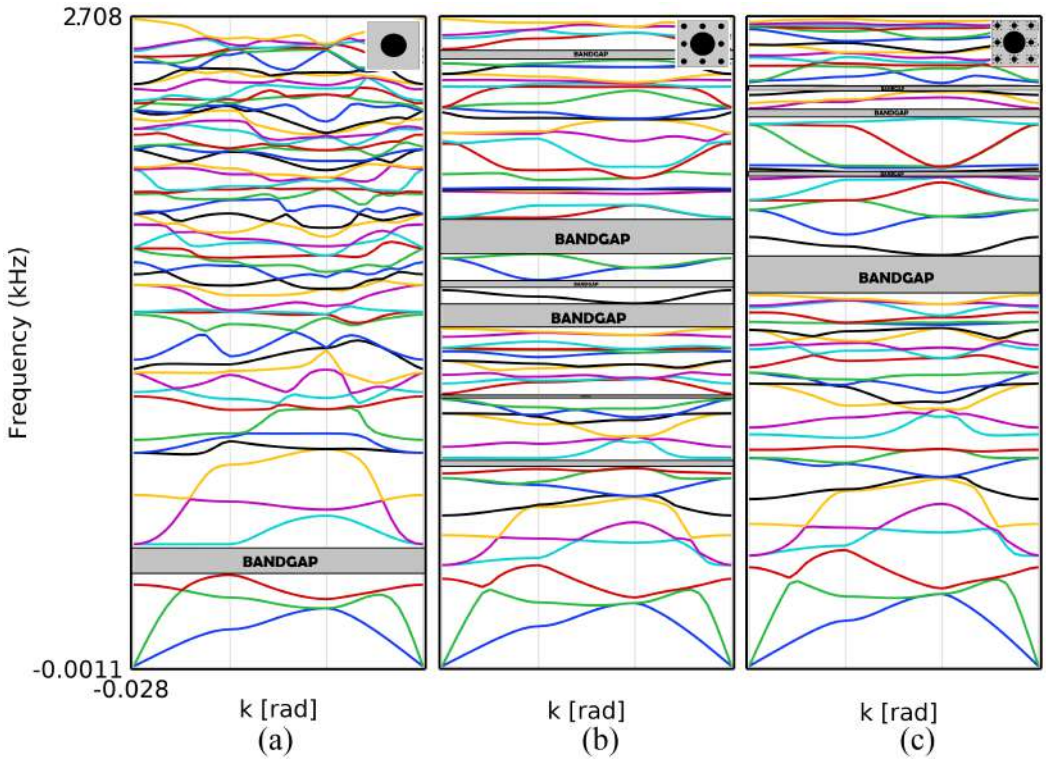

Figure 7. Band structure of phononic crystal fractal with quasi-Sierpinski distribution for cylinder inclusions.

For the second stage fractal, a different answer is found. The first low frequency bandgap continues to be eliminated when the filling fraction is increased and now two wider bandgaps appear: the first from 1425 to 1538 Hz and the second from 1733 to 1958 Hz. And three other bandgaps with a width small band at: 1115, 1638 and 2611 Hz.

In the third stage (Fig. 7 (c)), it is observed that the two wider bandgaps that appear at middle frequencies in Fig. 7 (b) disappear, having only a bandgap from 1610 to 1703 Hz. At high frequencies there is the existence of three more small bandgaps at: 2115, 2468 and 2654 Hz.

4. FINAL REMARKS

The PWE method was used to evaluate PC band structures with quasi-Sierpinski fractal distribution. At first, PWE was implemented only for the first stage of the fractal, the other stages are under development. A good convergence was observed, mainly for low frequencies between the responses obtained by PWE and FE COMSOL (responses validated with the work of Huang *et al.* (2017)). The influence of different fractal distribution stages was investigated, as well as the behavior of fractals from circular inclusions.

Fig. 6 and 7 show the relationship between the increase in the filling fraction and the presence of wider and larger bandgaps, since there was an increase from 1 to 5 bandgaps for the square inclusion case and to 4 for the inclusion cases Circular. For both cases, the filling fraction has a significant impact on the bandwidth and in frequencies of bandgaps. The increase in the PC filling fraction and the implementation of circular shapes were significant modifications and were observed in the band structure of the Sierpinski carpet.

5. ACKNOWLEDGEMENTS

The authors gratefully acknowledge the support of the Brazilian funding agencies CAPES (Finance Code 001), CNPq (Grant Reference Numbers 313620/2018 and 151311/2020-0), FAPEMA (Grant Reference Numbers 00857/19, 02730/19, 00824/20 and 00133/21) and FAPESP (Grant Reference Number 2018/15894-0).

6. REFERENCES

Assis, T.A.d.e.a., 2008. "Geometria fractal: propriedades e características de fractais ideais". *Revista Brasileira de Ensino de Física [online]*. doi:https://doi.org/10.1590/S1806-11172008000200005.

Bilal, O., Foehr, A. and Daraio, C., 2017. "Observation of trampoline phenomena in 3D-printed metamaterial plates." *Extreme Mechanics Letters*, Vol. 15, pp. 103–107.

H. Page, J., Yang, S., Liu, Z., Cowan, M., Chan, C. and Sheng, P., 2005. "Tunneling and dispersion in 3d phononic crystals". *Zeitschrift Fur Kristallographie - Z KRISTALLOGR*, Vol. 220, pp. 859–870. doi:10.1524/zkri.2005.220.9-10.859.

Huang, J., Shi, Z. and Huang, W., 2017. "Multiple band gaps of phononic crystals with quasi-sierpinski carpet unit cells". *Physica B: Condensed Matter*, Vol. 516, pp. 48–54. ISSN 0921-4526. doi:https://doi.org/10.1016/j.physb.2017.04.022. URL https://www.sciencedirect.com/science/article/pii/S0921452617301989.

Kuo, N.K. and Piazza, G., 2011. "Fractal phononic crystals in aluminum nitride: An approach to ultra high frequency bandgaps". *Applied Physics Letters*, Vol. 99. doi:10.1063/1.3651760.

Li, F., Wang, Y. and Zhang, C., 2018. "A bem for band structure and elastic wave transmission analysis of 2d phononic crystals with different interface conditions". *International Journal of Mechanical Sciences*, Vol. 144, pp. 110 – 117. ISSN 0020-7403. doi:https://doi.org/10.1016/j.ijmecsci.2018.05.042. URL http://www.sciencedirect.com/science/article/pii/S0020740318304971.

Liu, Y.H., Chang, C.C., Chern, R.L. and Chang, C.C., 2007. "Phononic band gaps of elastic periodic structures: A homogenization theory study". *Phys. Rev. B*, Vol. 75, p. 054104. doi:10.1103/PhysRevB.75.054104. URL https://link.aps.org/doi/10.1103/PhysRevB.75.054104.

Reha, Abdelati, E.A.A. and Bouchouirbat, M., 2018. "The behavior of cpw-fed sierpinski curve fractal antenna". *Journal of Microwaves, Optoelectronics and Electromagnetic Applications [online]*. doi:https://doi.org/10.1590/2179-10742018v17i31244.

Sigalas, M.M. and Economou, E.N., 1992. "Elastic and acoustic wave band structure". *Journal of Sound and Vibration*, Vol. 158, No. 2, pp. 377 – 382. ISSN 0022-460X. doi:https://doi.org/10.1016/0022-460X(92)90059-7. URL http://www.sciencedirect.com/science/article/pii/0022460X92900597.

Vasseur, J.O., Djafari-Rouhani, B., Dobrzynski, L., Kushwaha, M.S. and Halevi, P., 1994. "Complete acoustic band gaps in periodic fibre reinforced composite materials: the carbon/epoxy composite and some metallic systems". *Journal of Physics: Condensed Matter*, Vol. 6, No. 42, pp. 8759–8770. doi:10.1088/0953-8984/6/42/008. URL https://doi.org/10.1088%2F0953-8984%2F6%2F42%2F008.

Yao, Z.J., Yu, G.L., Wang, Y.S. and Shi, Z.F., 2009. "Propagation of bending waves in phononic crystal thin plates with a point defect". *International Journal of Solids and Structures*, Vol. 46, No. 13, pp. 2571 – 2576. ISSN 0020-7683. doi:https://doi.org/10.1016/j.ijsolstr.2009.02.002. URL http://www.sciencedirect.com/science/article/pii/S0020768309000699.

7. RESPONSIBILITY NOTICE

The authors are solely responsible for the printed material included in this paper.